



Many-body approximations to the superfluid gap and critical temperature in pure neutron matter

Mehdi Drissi^{1,3,a} , Arnau Rios^{2,3,b} 

¹ TRIUMF, 4004 Wesbrook Mall, Vancouver, BC V6T 2A3, Canada

² Departament de Física Quàntica i Astrofísica, Institut de Ciències del Cosmos (ICCUB), Universitat de Barcelona, Martí Franquès 1, Barcelona 08028, Spain

³ Department of Physics, University of Surrey, Guildford GU2 7XH, UK

Received: 15 February 2022 / Accepted: 21 April 2022 / Published online: 12 May 2022

© The Author(s) 2022

Communicated by L. Tolos

Abstract We compute singlet pairing gaps and critical temperatures in pure neutron matter with different many-body approximations. Medium effects tend to reduce gaps and critical temperatures compared to the standard BCS ansatz. In the mean-field approximation, the ratio of these two quantities remains constant across a wide range of densities. This constant ratio is close to the universal prediction of BCS theory, whether three-neutron interactions are included or not. Using a more sophisticated many-body approach that incorporates the effect of short-range correlations in pairing properties, we find that the gap to critical temperature ratio in the low-density regime is substantially larger than the BCS prediction, independently of the interaction. In this region, our results are relatively close to experiments and theoretical calculations from the unitary Fermi gas. We also find evidence for a different density dependence of zero-temperature gaps and critical temperatures in neutron matter.

1 Introduction

Neutron stars (NSs) are key astrophysical objects. Their existence depends on several predicted properties of matter at the extremes of density, temperature and isospin asymmetry [1,2]. In turn, the astrophysical properties of NSs may be used to constrain the properties of extreme matter and, one hopes, the underlying nuclear physics properties. The telltale example of how the connection between microscopic (nuclear) and macroscopic (astrophysical) properties can be established is the relationship between the Equation of State (EoS) of nuclear matter and the mass-radius relation of NSs. General relativity is required to compute NS structure [3],

typically implemented by means of the hydrostatic, spherically symmetric and non-rotating Tolman–Oppenheimer–Volkov (TOV) equations. These equations require as input the EoS of dense matter, usually in the form of a nuclear physics inspired, one-to-one relation between energy density and pressure [4]. The solution of the TOV equations, in turn, provides a mass-radius relation for NSs, which can be immediately compared to observations [5,6]. In the current era of multi-messenger astrophysics, there is an ever increasing set of available NS data, including tens of pulsar masses from radio sources [7–9]; a handful of radii from X-ray observations [6,10,11]; and tidal deformabilities from gravitational waves [12–14]. Ultimately, the expectation is that a meaningful comparison between predictions and observations can constraint the available space of EoSs and, with it, the underlying nuclear models to generate them. As a starting step in this long-term endeavour, several EoS compilations are already available [15,16], providing a useful starting point for data-theory comparisons. The CompOSE database is one of such EoS compilations, focusing (not exclusively) on finite-temperature effects for supernova simulations [17].

While the mass-radius relation is a holy grail of NS physics, there are other aspects of NSs that are of general astrophysical interest. Nuclear many-body theory indicates that neutrons undergo spontaneous pairing in the crust and outer core of the star [18,19], much as they do in nuclei [20]. The existence of a superfluid phase may affect the dynamics of the star. For example, the observation of period glitches of pulsars are often interpreted as an abrupt transfer of angular momentum from superfluid matter to the rest of the star [21]. Similarly, the superfluid pair-formation mechanism of relatively young pulsars may accelerate their cooling [22–28]. These observations provide an insight beyond the EoS of NS dense matter, with the tantalising potential to elucidate dif-

^a e-mail: mldrissi@triumf.ca

^b e-mail: arnau.rios@icc.ub.edu (corresponding author)

ferent microphysical mechanisms at play in the interior of the star.

Like the EoS, the superfluid properties of a NS are theoretical predictions based on a given set of ingredients and approximations. Several predictions of the pairing gaps are available in the literature [20,29,30]. Some of these have been reduced to simple numerical parametrizations for ease of practice [31], although no universal database is currently employed. In practice, in the astrophysical context, EoS and superfluid gaps are often exploited independently of their origin. In doing so, one may mix together predictions that are based on very different nuclear physics models. These inconsistencies are often disregarded, because the final astrophysical observations may not always have enough resolving power to distinguish among different scenarios. But, as the quantity and quality of astrophysical data influenced by superfluidity increases, a reduction of the parameter space is likely to provide more stringent constraints. Theoretical consistency is imperative if the ultimate goal is to provide a propagation of information from astrophysical observations all the way down to nuclear physics [32].

Here, we identify and quantify one specific obstacle in this direction. More specifically, we examine an approximation employed in the astrophysical context that is not necessarily justified in terms of nuclear many-body theory. We look at the relation between the size of the zero-temperature superfluid gap, $\Delta_0 = \Delta(T = 0)$, and the critical temperature, T_c , of the superfluid transition. Hereafter, we work with the choice of units $\hbar = k_B = 1$. In the simple Bardeen–Cooper–Schrieffer (BCS) model of superconductivity, one finds that the ratio of these two quantities is independent from the strength of the interaction, from the density of the medium as well as from the cut-off of the regulator. In this case, the universal ratio simply is $\Delta_0/T_c = \pi/e^\gamma \approx 1.764$ [33]. This remarkable result, or its corresponding extension to the triplet case [34–37], is exploited throughout the NS literature [22,31].

In the following, we explore whether this BCS prediction of a constant Δ_0/T_c ratio remains valid for the singlet gap in the NS context. There are reasons to believe that this may not be the case. First of all, the impact of the medium on the pairing gap is sizeable and non-trivial in neutron matter [20,38]. At the simplest possible level, nucleon propagation is modified by a mean field potential. Beyond this mean-field picture, more sophisticated many-body approximations also predict a substantial modification of single-particle strength. Second, and equally relevant, the nucleonic interaction is far from the simple one considered in the BCS model. In particular, three-neutron forces (3NF) are important at nuclear densities, and their appearance is known to modify the pairing gap at zero temperature [39]. We look at whether such modifications can affect the pairing gap, the critical temperature and their ratio.

More fundamentally, the BCS many-body approximation can be interpreted as the lowest-order of a many-body expansion in the context of superfluids. Since the expansion parameter in this case is the strength of the potential, one may question whether expectations from BCS predictions are reliable anymore in the strongly interacting, high-density regime of neutron stars. Along these lines, one can foresee two different types of medium modifications. In one instance, the gap Δ_0 and the critical temperature T_c may be modified, while keeping their ratio Δ_0/T_c intact. This probably requires some cancellations or fine tuning, which operate at the BCS level and, possibly, beyond. Alternatively, the medium modifications may change both Δ_0 and T_c in a way that their ratio is modified. This scenario has already been realised in several instances in ultracold gases and high- T_c superconductors, where the ratio Δ_0/T_c deviates substantially from the BCS prediction [40–44].

Chiral effective field theory interactions among nucleons provide a solid starting point to explore the properties of dense neutron matter in the region of interest for singlet pairing superfluidity, up to and around saturation density [45,46]. Importantly, by looking at the cutoff and scheme dependence, one can quantify to some extent the theoretical uncertainty of neutron-matter properties [47]. Interactions are only the starting point, though. For dense matter studies, one also needs to resort to a many-body scheme that provides an approximate solution for the thermodynamics and the superfluid properties. Many different methods exist to address specifically the EoS problem, both at zero and finite temperature [48–50]. When it comes to superfluidity, however, one typically works in a BCS approach, with some minor modification [20,35,36,51]. Extensions beyond the BCS level are typically phenomenological in nature [52–54], or cannot easily be systematized to provide theoretical uncertainties [38,55–57].

Recently, we have formulated a new theoretical framework that addresses this issue and facilitates the systematic exploration of many-body effects in superfluid systems at finite temperature [58,59] framework, dubbed Nambu-Covariant Green's Functions, develops a diagrammatic expansion that can potentially provide predictions for many-body scheme uncertainties. Importantly, the theory can also be used to build self-consistent approaches and hence provide a simplified superfluid counterpart to the more conventional self-consistent Green's function (SCGF) approach [60,61]. The numerical implementation of this Nambu-covariant Green's function method is not yet available. While this is developed, we explore here an alternative approach based on previous SCGF work [38,57,62]. We include the effect of short-range correlations (SRC) effectively in the pairing gap by modifying the superfluid gap equation with convolutions of normal propagators. We study both the gap and the critical temperature calculations, to pro-

vide an initial assessment of the modifications of the Δ_0/T_c ratio in dense matter. While this approach is not yet entirely consistent, we find a strong modification of the ratio even in the low-density regime. Exploring the astrophysical implications of these findings will require the full development of new techniques in the future.

We now proceed to discuss the two different many-body approximations that we employ to compute the pairing gap, in an effort to provide an estimate of theoretical uncertainties. We also provide parametrizations for the gap and the critical temperature dependence on Fermi momentum, in an attempt to assess whether these dependences are the same or not. We first introduce the BCS approach with a Hartree-Fock (HF) single-particle spectrum, and discuss finite-temperature results. Then, we discuss a finite-temperature extension of the SCGF model that can incorporate the effects of short-range correlations effectively in the superfluid phase. This extension was originally introduced in Ref. [62] and further developed at zero temperature in Refs. [38,57]. The results presented here represent the first systematic exploration of this method across a wide range of temperatures. Our discussion is restricted to the singlet gap in the 1S_0 channel, but the extension to an angle-averaged triplet case is relatively straightforward.

2 Bardeen-Cooper-Schrieffer pairing

The momentum-dependent superfluid gap at a given temperature can be computed from an integral gap equation, which has the generic structure

$$\Delta_k = - \int \frac{dk'}{(2\pi)^3} \frac{\mathcal{V}(k, k')}{2\chi_{k'}} \Delta_{k'}. \tag{1}$$

Here, Δ_k is the singlet pairing gap that one is interested in, which appears in both sides of the equation. Within the BCS approximation, $\mathcal{V}(k, k')$ is the bare NN interaction in the 1S_0 partial wave for the singlet pairing case of interest here. k and k' are, respectively, the incoming and outgoing relative momentum of a pair. The standard BCS kinematics involves a zero center-of-mass momentum [20].

The energy denominator χ_k contains information on the superfluid pairs, including the gap itself as well as the temperature of the system. In a standard BCS approximation, the denominator is

$$\frac{1}{2\chi_k} = \frac{1 - 2f(\xi_k)}{2\xi_k}, \tag{2}$$

with $f(\omega) = [1 + \exp(\frac{\omega - \mu}{T})]^{-1}$ a Fermi-Dirac distribution. The quasi-particle energies are defined by

$$\xi_k = \sqrt{(\varepsilon_k - \mu)^2 + \Delta_k^2}, \tag{3}$$

where Δ_k denotes the gap contribution, μ is the chemical potential, and ε_k , the single-particle spectrum.

Different approximations to ε_k provide different pairing gaps. The standard BCS approach uses only a crude kinetic dispersion relation, $\varepsilon_k = k^2/2m$. One step towards a more realistic description is to dress this dispersion relation with a mean-field Σ_k ,

$$\varepsilon_k = \frac{k^2}{2m} + \Sigma_k. \tag{4}$$

This is motivated theoretically by the well-known Hartree-Fock-Bogoliubov approach [63]. The mean-field incorporates the average effect of interactions in the medium,

$$\Sigma_k = \int \frac{dk'}{(2\pi)^3} \langle \mathbf{k}\mathbf{k}' | V | \mathbf{k}\mathbf{k}' \rangle_A n'_k. \tag{5}$$

Here, the interaction matrix elements are antisymmetrized and \mathbf{k} and \mathbf{k}' represent single-particle momentum vectors. At the BCS level, the pairing interaction $\mathcal{V}(k, k')$ is related to the matrix elements $\langle \mathbf{k}_1 \mathbf{k}_2 | V | \mathbf{k}'_1 \mathbf{k}'_2 \rangle_A$ by setting $\mathbf{k}_1 = -\mathbf{k}_2 = \mathbf{k}$ and $\mathbf{k}'_1 = -\mathbf{k}'_2 = \mathbf{k}'$ and expanding to the appropriate partial wave.

The momentum distribution in the superfluid case is given by the expression

$$n_k = 1 - \frac{\varepsilon_k - \mu}{\xi_k} \tanh\left(\frac{\xi_k}{2T}\right). \tag{6}$$

At each Fermi momentum, $k_F = (3\pi^2\rho)^{1/3}$, we find the corresponding chemical potential by inverting the expression

$$\rho = 2 \int \frac{dk}{(2\pi)^3} n_k. \tag{7}$$

This already departs from the standard BCS approach, which employs $\mu = \varepsilon_F = k_F^2/2m$. This determination of μ is more consistent with the Hartree-Fock-Bogoliubov picture in the canonical ensemble, and with other many-body approximations [64–66]. Compared to the standard BCS approach, this canonical implementation yields a small reduction of the gap in the low-density regime.

One of the key advantages of chiral interactions is that each order in the expansion gives rise to associated many-body forces [45]. These become more relevant as the density of the system increases. In the predictions shown here, we use the N3LO Entem-Machleidt (EM) interaction V_{NN} [67] and supplement it with a three-nucleon force (3NF) W at N2LO. We use $\Lambda = 500$ MeV in both cases. The 3NF are incorporated following Refs. [68–70], using the $P = 0$ approximation and an internal nonlocal regulator. We contract W with the momentum distribution of Eq. (6) to obtain an effective two-body force, \tilde{W} . Carefully considering the

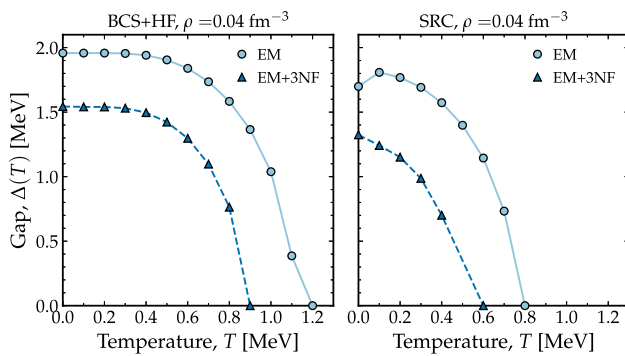


Fig. 1 Left panel: superfluid gap Δ as a function of temperature T in the BCS+HF approximation. Circles (triangles) correspond to results with the EM force (EM+3NF) force. Right panel: the same for results using the SRC approximation

normal ordering of each contribution, one finds that in the calculation of the single-particle mean-field, Σ , one needs to employ the sum $V = V_{NN} + \frac{1}{2}\tilde{W}$. In contrast, in the pairing gap $\mathcal{V} = V_{NN} + \tilde{W}$ [39,58,59]. We compute the Hartree-Fock self-energy numerically with partial waves up to a total angular momentum of the neutron pair $J = 10$.

Because μ enters both the gap equation and the momentum distribution, the BCS+HF gaps and quasi-particle energies need to be computed iteratively. At each density and temperature, one can iterate Eqs. (1)–(4) to find a solution for the momentum dependent mean-fields, Σ_k , and gap functions, Δ_k . As temperature increases, smearing out the Fermi surface, one expects the gap to decrease until it disappears at a given T_c . We explore this phase transition by simulating several temperatures for a given density (or Fermi momentum) value, as shown in Fig. 1. The left panel shows the pairing gap at $k = k_F$, $\Delta(T)$, for a density $\rho = 0.04 \text{ fm}^{-3}$ and varying temperatures, T . As temperature increases, the gap decreases monotonically until it eventually disappears for a given critical temperature. The resolution of T_c is limited by the numerical mesh. For the EM results only (full circles) shown in Fig. 1, T_c lies between 1.1 and 1.2 MeV. We thus estimate the critical temperature at this density as $T_c = 1.15 \pm 0.05$ MeV. The inclusion of repulsive 3NF generally decreases the pairing gap. The EM+3NF results shown with triangles (dashed lines) are indeed lower across the whole temperature range. The pairing gap decays faster with 3NFs as a function of temperature, and the corresponding critical temperature is $T_c = 0.85 \pm 0.05$ MeV. We stress that these results incorporate a temperature-dependent single-particle spectrum Σ , with 3NFs that are consistently included in the pairing interaction. This complicates the potential application of alternative methods that estimate T_c using algorithms relying on the Thouless criterion, like the Weinberg eigenvalue approach used in Ref. [71].

One can proceed similarly for different densities, generating a mesh of gap values for different thermodynamical conditions. With this, one gets the results displayed in Fig. 2. The top panel shows the zero-temperature gap, Δ_0 , as a function of Fermi momentum. We show three different sets of results. The dashed line is a reference standard BCS value, obtained with the EM NN interaction only; a non-interacting single-particle spectrum, i.e. $\Sigma = 0$; and a chemical potential $\mu = \varepsilon_F$. In contrast, the circles and triangles joined by a full line correspond to EM BCS+HF results ($\Sigma \neq 0$) with (triangles) or without (circles) 3NFs. In these results, the chemical potential is determined using Eq. (7).

The gaps show the standard dumbbell shape for all cases. The position and size of the maximum gap depends on the many-body scheme. For the EM BCS results, the gap maximum is close to 3 MeV at $k_F = 0.9 \text{ fm}^{-1}$. The BCS+HF results have in general lower gap values, with a maximum around ≈ 2.7 MeV at a Fermi momentum of $\approx 0.8 \text{ fm}^{-1}$. As density increases beyond the peak, the gap subsequently decreases and closes near $1.4 - 1.5 \text{ fm}^{-1}$ for the BCS+HF simulations, and around 1.6 fm^{-1} for the BCS-only case. The effect of the 3NF is to reduce the maximum gap by about 0.2 MeV, and also to bring the gap closure to lower densities. This effect is well-known and has already been identified in BCS and in BCS+HF calculations [38,39]. Our results also coincide with those generated by Drischler et al. in Ref. [39].

While the symbols in Fig. 2 represent the numerical simulations, the lines have been obtained by fits to the data with the function

$$g^x(k_F) = g_0^x \frac{(k_F - k_0^x)^2}{(k_F - k_0^x)^2 + k_1^x} \frac{(k_F - k_2^x)^2}{(k_F - k_2^x)^2 + k_3^x}, \quad (8)$$

with $g_0^x, k_0^x, k_1^x, k_2^x$ and k_3^x numerical parameters [31]. Here, x labels the data that is fitted, with $x = \Delta_0$ for pairing gaps and $x = T_c$ for critical temperatures. Details on the numerical fit to this function are given in Appendix A. We note that the fits provide a very good reproduction of the BCS results, with maximum deviations with respect to data of 0.04 MeV across the whole density regime. The top rows of Table 1 provide the corresponding fit parameters for the pairing gaps. k_0^Δ and k_2^Δ represent the Fermi momenta at which the gap opens and closes, respectively. The opening Fermi momentum is the same for both the EM and EM+3NF calculations, as expected naively from the growing importance of 3NFs with density. In contrast, the fit indicates that the closing Fermi momentum for the singlet gap without 3NFs, $k_2^\Delta = 1.49 \text{ fm}^{-1}$, is larger than the EM+3NF result, $k_2^\Delta = 1.37 \text{ fm}^{-1}$.

The central panel in Fig. 2 shows T_c as a function of Fermi momentum, obtained as explained earlier by computing the gap at different temperatures. Because of the limited numerical mesh of temperatures, we assign an error to T_c , which is typically $\varepsilon_{T_c} = 0.05$ MeV or, on occasions, 0.1 MeV.

Table 1 Parameters generated by a fit to the calculated gaps, Δ_0 (top 2 rows), and the critical temperatures (bottom 2 rows). These results correspond to the BCS+HF approximations

BCS+HF Units	g_0^Δ MeV	k_0^Δ fm^{-1}	k_1^Δ fm^{-2}	k_2^Δ fm^{-1}	k_3^Δ fm^{-2}
EM	24.76	0.02	1.23	1.49	0.89
EM+3NF	15.09	0.02	1.02	1.37	0.62
	$g_0^{T_c}$	$k_0^{T_c}$	$k_1^{T_c}$	$k_2^{T_c}$	$k_3^{T_c}$
EM	7.30	0.02	0.92	1.48	0.69
EM+3NF	7.94	0.01	1.00	1.37	0.59

The data has a very similar shape to the BCS+HF zero-temperature gap - a dumbbell, with a maximum of ≈ 1.5 MeV at around $k_F \approx 0.8 \text{ fm}^{-1}$. T_c decreases at high density, until it closes around 1.4 fm^{-1} . BCS results without HF spectra (dashed lines) predict substantially larger critical temperatures. To quantify the similarity between the shape of the gap parameter and the critical temperature, we fit the function of Eq. (8) to the T_c data, considering the theoretical uncertainty. We provide the fit parameters in the bottom rows of Table 1. Looking again at the opening and closing Fermi momenta, $k_0^{T_c}$ and $k_2^{T_c}$, we find a very good agreement between the gap and the critical temperature data. The comparison between the values of k_1^x and k_3^x can only be done in relative terms. We find that the ratio k_1^x/k_3^x for the gap and T_c fits with the EM interaction are close to each other, $k_1^x/k_3^x = 1.3-1.4$. For the EM+3NF fits, the fits provide two consistent ratios $k_1^x/k_3^x = 1.6-1.7$, which are different to the EM ones. These ratios illustrate the faster decline with Fermi momentum of the EM+3NF results as opposed to the EM-only ones. With this in mind, we conclude that the gap and the critical temperature are different for different interactions, but they have essentially the same dependence in k_F within the BCS+HF approximation.

Finally, the bottom panel of Fig. 2 shows the results for the ratio of the gap to the critical temperature values, Δ/T_c . The bands correspond to the (independent) uncertainty propagation of the errors associated to the gap (negligible at the BCS+HF level) and the critical temperature (of order $\epsilon_{T_c} = 0.05$ MeV, as stated above). We raise at least two relevant astrophysical conclusions from this result. First, the ratio is obviously quite constant over a wide density regime. This supports the statement in the previous paragraph that the functional forms of $\Delta_0(k_F)$ and $T_c(k_F)$ are very similar in the BCS+HF approximation. Second, the ratio does coincide with the BCS result, $\Delta_0/T_c = 1.764$ [33] within the uncertainties generated by our results which are of the order of 0.1. The deviations from the universal constant are commensurate with this uncertainty and there are no clear trends nor departures from this value.

We stress that the results presented here, within the BCS+HF approach (solid lines), go beyond the standard BCS (dashed line) approximation that is used to derive the identity $\Delta_0/T_c = 1.764$. This result arises from an analysis of the kernel of Eq. (1) close to $T = 0$ and close to T_c . The standard analysis neglects the effects of the momentum dependence (or the non-locality) of the interaction, and is performed in the absence of 3NFs. Likewise, the analysis typically neglects the single-particle mean-field, $\Sigma = 0$. Here, instead, Σ is momentum, density and temperature dependent at the HF level. 3NFs affect the pairing properties both through Σ itself, but also through the pairing interaction, \mathcal{V} . And, yet, even though these changes do substantially modify the values of Δ_0 and T_c independently (see top and central panels), our results indicate that the ratio Δ_0/T_c is independent of all such medium modifications.

3 Beyond-BCS pairing

We now apply the very same methodology in an approximation that goes beyond the BCS+HF approximation. We aim to test whether the ratio Δ_0/T_c can be modified, but we also want to quantify the deviation from the BCS+HF results. To this end, we implement an approximation that incorporates the fragmentation of quasi-particle strength effectively in the pairing properties [38, 57, 62]. The single-particle spectral function, $A_k(\omega)$, provides a positive-definite probability distribution which describes the fragmentation of strength for a given momentum, k , in the normal state [72, 73]. In a mean-field approximation, such as HF, this is just a δ peak centered at a certain effective single-particle energy ϵ_k . Going beyond mean-field approximations, however, the spectral functions departs from this basic δ distribution [72, 73].

In the SCGF approach at finite temperature, $A_k(\omega)$ is instead a density and temperature-dependent function, with a strong peak around a preferred single-particle energy, but also relatively large widths beyond the Fermi surface [61].

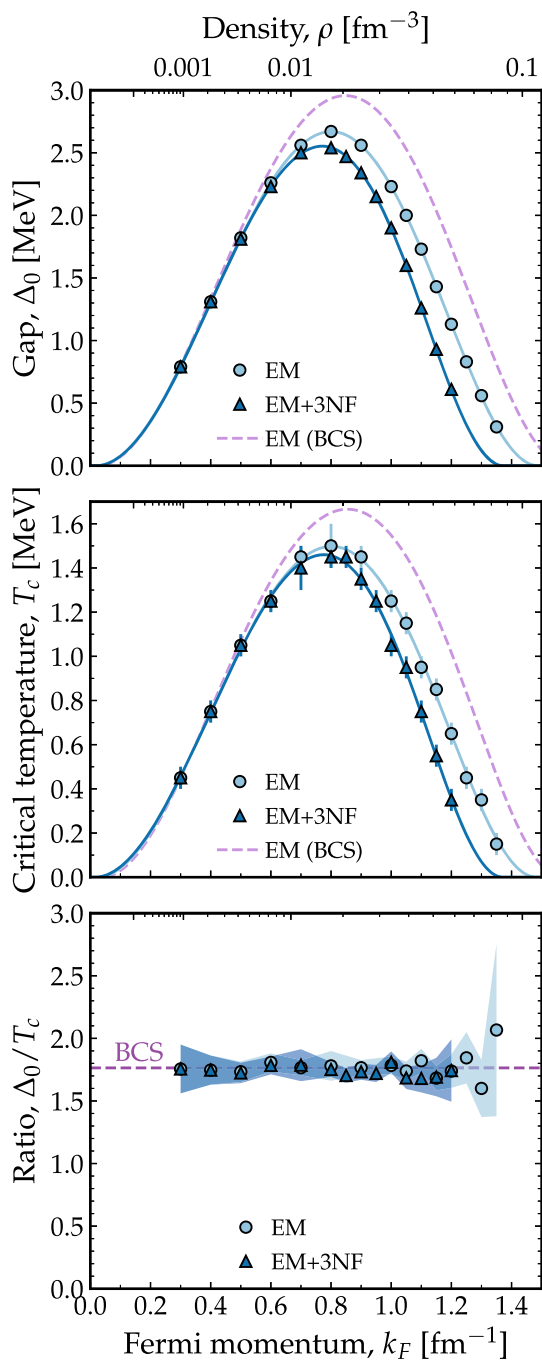


Fig. 2 Top panel: zero-temperature superfluid gap Δ_0 as a function of neutron matter Fermi momentum. Filled circles (triangles) represent the BCS+HF solution for the N3LO EM (N3LO+3NF) potential. Dashed lines correspond to the BCS solution for the EM interaction. Central panel: critical temperature T_c as a function of neutron matter Fermi momentum. The error bars represent the numerical uncertainty in the determination of T_c . The symbols have the same meaning as the top panel. Bottom panel: ratio of T_c to Δ as a function of Fermi momentum. The dashed horizontal line is the BCS result $\Delta_0/T_c = 1.764$

We access the spectral function by means of finite temperature SCGF calculations [38,61,69]. For any given density and temperature, a SCGF simulation sums an in-medium (particle-particle and hole-hole) ladder series at finite temperature [74,75]. For a fixed ρ , we can perform simulations for several values of T , down to minimum temperatures of order 2 MeV, well above any pairing instability [76]. With this data, we can extrapolate below the minimum temperature value and obtain a normal spectral function in a regime which may be superfluid, as explained in Ref. [57]. This extrapolation allows us to compute a fragmented pairing contribution to the denominator,

$$\frac{1}{2\zeta_k} = \int \frac{d\omega}{2\pi} \frac{d\omega'}{2\pi} \frac{1 - f(\omega) - f(\omega')}{\omega + \omega'} A_k(\omega) A_k(\omega'), \quad (9)$$

so that $\chi_k = \sqrt{\zeta_k^2 + \Delta_k^2}$ in the pairing gap equation, Eq. (1) [62]. We note that the extrapolation procedure only works for systems which are relatively degenerate or, in other words, for relatively large densities, above $k_F \approx 0.6 \text{ fm}^{-1}$.

The extrapolated pairing denominator χ_k can be directly employed in the gap equation, Eq. (1). We stress, however, that many-body theoretical approaches indicate that the integral convolution should also include one superfluid (as opposed to normal) spectral function [77]. In other words, we are missing feedback effects from the superfluid into the gap itself. These effects occur very close to the Fermi surface and are expected to be relatively small [62]. In the absence of the full implementation of a consistent many-body theory of superfluids, as presented in Refs. [58,59], we use this approach as an initial step forward in the analysis.

SRC associated with realistic NN forces induce fragmentation on spectral functions. This fragmentation reduces the pairing gap [62,74]. Our simulations corroborate this conclusion at finite temperatures. The right panel of Fig. 1 shows SRC pairing gaps as a function of temperature for EM (circles) and EM+3NF (triangles). The SRC gaps are smaller than their BCS+HF counterparts across the whole temperature regime. Importantly, the temperature dependence of these results is steeper, and the corresponding critical temperatures are substantially reduced. We note that the $T = 0$ temperature result for the EM interaction deviates from the monotonous dependence obtained with the finite-temperature results. This is most likely an artefact of the numerical extrapolation procedure. In the following, we associate a constant theoretical uncertainty, $\epsilon_{\Delta_0} = 0.1 \text{ MeV}$, to our results, to account for such issues. In the case of EM+3NF, this error also incorporates the uncertainty associated to the fact that the reduction of the 3NF into an effective 2-body force is performed with a step-function momentum distribution, n_k , as opposed to the pairing-corrected distribution of Eq. (6).

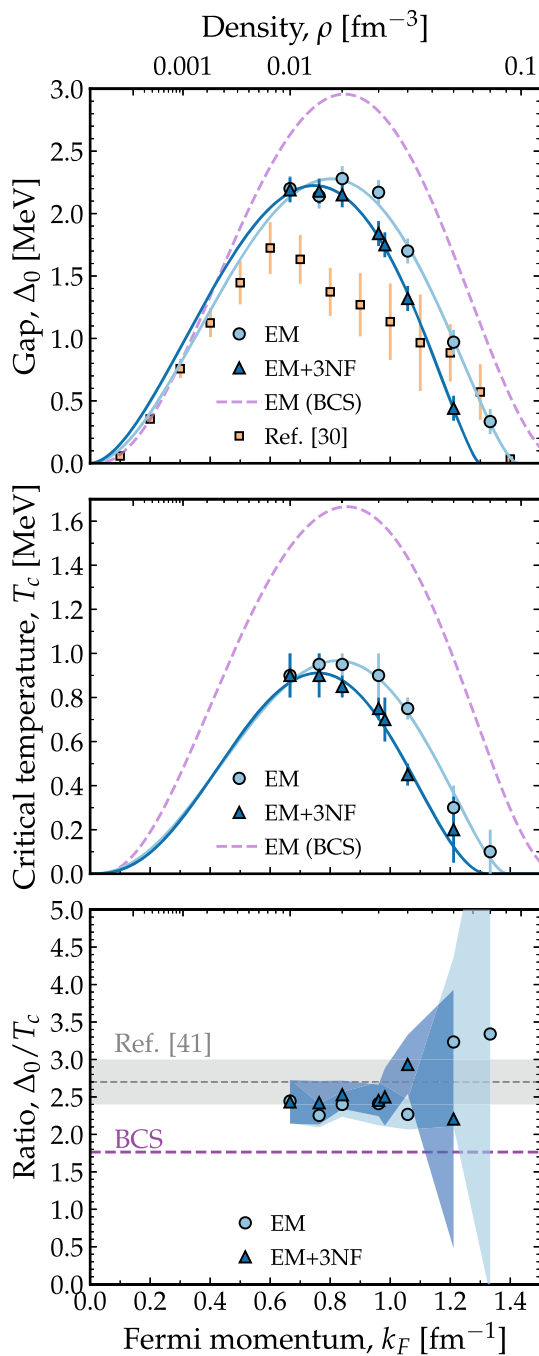


Fig. 3 The same as Fig. 2 for the SRC approximation

We present the results for Δ_0 in the SRC for the EM (circles) and the EM+3NF (triangles) interactions in the top panel of Fig. 3. This figure also includes the BCS results (dashed line). Compared to Fig. 2, the SRC results provide smaller gaps across the whole density regime, with maximum gaps here of order 2.4 MeV. Just as in the BCS+HF case, 3NFs tend to reduce the maximum gap and the closure Fermi momentum further. We provide the associated fits to this data in Table 2. These fits suggest that the gap opens at zero Fermi

momentum, $k_0^\Delta = 0 \text{ fm}^{-1}$. This is the lowest bound imposed in our fitting procedure. We stress, however, that the lack of SRC data in the region below the peak does not help in constraining the low-density parameters. The closure gap Fermi momentum, k_2^Δ , in contrast, is better determined and relatively close to the BCS+HF results.

We show in the top panel of Fig. 3 (squares) recent gap results obtained with quantum Monte Carlo (QMC) techniques in Ref. [30]. These results are based on the Av8' interaction supplemented with the Urbana-IX three-body force. For Fermi momenta $k < 0.4 \text{ fm}^{-1}$, the agreement between the extrapolated SRC and QMC results is remarkable. QMC results peak at a somewhat lower value of $\Delta_0 \approx 2 \text{ MeV}$, a discrepancy that could be due to the difference in interactions, in many-body schemes or both. While the intermediate density dependence is different, we note that there is an agreement in the closure Fermi momentum, which is around $k_F \approx 1.4 \text{ fm}^{-3}$ for both the QMC and the SRC predictions with the EM interaction.

The central panel of Fig. 3 shows the critical temperature obtained in the SRC approach. The maximum T_c for both the EM and the EM+3NF in this approach is below 1 MeV. This represents a decrease of 0.5 MeV with respect to the BCS+HF data in the central panel of Fig. 2. This is also 0.7 MeV lower than the maximum T_c of the BCS-only approximation. While the error bars in the plot are not negligible, with a few points with $\epsilon_{T_c} = 0.1 \text{ MeV}$, they do allow for a numerical fit. The results, presented in the bottom rows of Table 2 indicate that T_c may vanish at a Fermi momentum which is around 0.05 fm^{-1} lower than the corresponding gap closure parameter.

Astrophysical applications, like cooling curve simulations, rely on parametrizations of the density dependence of T_c , which is often assumed to be the same as that of the gap, Δ . The results of our SRC fits indicate that the functional forms of the gap and the critical temperature fits may be quite different. For the EM force, for instance, the ratio of fit gap parameters is $k_1^\Delta/k_3^\Delta \approx 1.4$, whereas the corresponding T_c fit yields $k_1^\Delta/k_3^\Delta \approx 1.9$. A similar conclusion is drawn with EM+3NF, thus indicating that the functional dependences are rather dissimilar.

The main results of this paper are presented in the bottom panel of Fig. 3. We report on the ratio of the gap to the critical temperature within the SRC approach. The bands associated to the data incorporate the errors in both the gap and the critical temperature, propagated assuming that they are independent to each other. In addition to the BCS ratio (dashed line), the figure shows the prediction $\Delta_0/T_c = 2.7 \pm 0.3$ from Ref. [41]. This band is extracted from a functional renormalization group analysis applied to the unitary Fermi gas. This comparison is of interest because of the un-naturally large S-wave scattering length displayed by neutrons in the vacuum. Neutron matter can thus be interpreted as a deviation from the standard unitary Fermi gas. The band obtained in Ref. [41] is

Table 2 The same as Table 1 for the SRC approximation

SRC Units	g_0^Δ MeV	k_0^Δ fm^{-1}	k_1^Δ fm^{-2}	k_2^Δ fm^{-1}	k_3^Δ fm^{-2}
EM	5.87	0.00	0.67	1.46	0.47
EM+3NF	5.04	0.00	0.57	1.35	0.39
	$g_0^{T_c}$	$k_0^{T_c}$	$k_1^{T_c}$	$k_2^{T_c}$	$k_3^{T_c}$
EM	2.53	0.00	0.74	1.40	0.39
EM+3NF	2.98	0.00	0.77	1.30	0.42

commensurate with other predictions from different many-body approaches. This band is also close to a ratio of independent experimental values for $\Delta_0 = 0.44(3)\epsilon_F$ [78] and $T_c = 0.167(13)\epsilon_F$ [79], which yields $\Delta_0/T_c = 2.63 \pm 0.27$ [80].

The data obtained within the SRC approach in the low Fermi momentum regime, $k_F < 1 \text{ fm}^{-1}$, is consistent with a ratio value of $\Delta_0/T_c = 2.4 \pm 0.3$. This is substantially larger than the BCS result, which is excluded even when considering theoretical errors in the gap and the critical temperature. We stress that there are substantial differences in gap and critical temperature values between the EM and the EM+3NF, but the ratio predictions in the region $k_F = 0.6 - 1.0 \text{ fm}^{-1}$ are extremely uniform. In particular, the ratio is insensitive to the inclusion of 3NFs. We have performed the same analysis for the CD-Bonn interaction, not shown here for brevity, and find also a good agreement in the ratios. Overall, this indicates that the ratio value due to the SRC method is robust.

The behaviour at higher densities is more difficult to pin down. We have access to only a few data points and the associated errors increase substantially as T_c decreases. The central values for the EM-only results indicate an increase in the ratio as the gap closure is reached. The results with 3NF at high densities are inconclusive, with one point lying above and another below 2.4. Overall, however, there are clear indications of deviations from the BCS ratio across a wide set of densities when using the SRC approach. A density-independent constant ratio could be straightforwardly implemented in cooling simulations [22,25], before the more sophisticated density dependence shown in Fig. 3 is explored. The analysis of how such a renormalization of this ratio, or even how different functional forms of Δ_0 and T_c would affect astrophysical simulations, lies beyond the exploratory nature of this work.

4 Conclusions and outlook

In this paper, we have critically assessed the singlet superfluid gap and the superfluid critical temperature in neutron matter. We review whether often-used assumptions in astrophysical

simulations, like the constant ratio between the critical temperature and the pairing gap predicted by BCS theory, hold in many-body schemes that go beyond BCS. To this end, we investigate two different avenues that go beyond standard BCS theory. The first one, close to the HFB approach, incorporates medium effects through a Hartree-Fock mean-field, Σ . The gap is informed of 3NFs through this mean-field, but also through an averaged effective two-body contribution to the pairing interaction. We find that medium effects, incorporated in this fashion, reduce substantially both the pairing gap and the critical temperature compared to the standard BCS approach. This reduction, however, does not modify the ratio Δ_0/T_c , which remains constant across densities and very close to the BCS universal prediction. We conclude that the medium modifications associated to the BCS+HF approach operate effectively in the same direction in both quantities, cancelling each other.

In contrast, the SRC approach to superfluid properties considers a more sophisticated approach to medium modifications. It incorporates an extrapolation of normal spectral functions to low temperatures and accounts for the fragmentation of single-particle strength. We find, in agreement with previous studies, that the pairing gap is reduced by SRCs. The critical temperature is computed here extensively for the first time, and we find it is also substantially reduced by SRC, compared to BCS or BCS+HF expectations. The maximum lies below $T_c = 1 \text{ MeV}$ across the whole density regime. Numerical fits to our data suggest that the functional form of T_c as a function of k_F may be relatively different to that of Δ_0 . In the low-density region, $k_F < 1 \text{ fm}^{-1}$, we find a universal value of the ratio $\Delta_0/T_c = 2.4 \pm 0.3$. This is substantially larger than the BCS prediction, but bodes well with theoretical simulations and experimental data for Δ_0 and T_c of the unitary Fermi gas.

In terms of future outlook, we differentiate between three different, yet interconnected, aspects: developments of the SRC approach; quantum many-body theory extensions; and their astrophysical impact. The SRC approach that we have just presented can be straightforwardly extended to other pairing scenarios and, in fact, it has already been used to predict triplet pairing gaps at zero temperature [38,57]. One

could use this approach to test whether the triplet gap-to- T_c ratio is also modified with respect to the BCS prediction. Extending the extrapolation procedure to arbitrary isospin asymmetry would also allow to explore similar effects in the more astrophysically relevant case of β -equilibrated matter and, in particular, would allow us to provide predictions for proton superconductors. It would be interesting to explore how NS thermal properties are modified using the SRC results presented here. This includes, for instance, the specific heat of neutron-star matter and other important transport coefficients.

Having said that, the relatively large errors of our numerical data are limiting the accuracy of our conclusions, and also hamper further inferences at high densities. Further improvements may require a new approach that actually accesses superfluid properties from the outset. We know, for instance, that there are missing aspects of the SRC approach that certainly modify Δ_0 , and can potentially alter the Δ_0/T_c ratio. Key among these is the effect of long-range correlations in the pairing interaction, which was explored in Ref. [57] in a phenomenological approach [52,54,81] and seen to further reduce the singlet pairing gap. Moreover, the double convolution denominator in the SRC approach does not fully account for superfluid properties and improvements of many-body theory are necessary at that level. Ideally, these many-body improvements should have associated uncertainties not only from the NN and 3NF (say, from the chiral expansion), but also from the many-body truncation scheme. In this sense, the ideal way forward is the recently developed Nambu covariant formalism of Refs. [58,59], a theoretical formalism that fulfills all the necessary conditions to provide predictions in this regime.

While quantum many-body theory developments occur, one can potentially explore the relevance of these results in astrophysical simulations. The fits we provide here can be directly adopted in cooling simulations performed with consistent EoS, to explore whether the reduction of T_c or, indeed, the change of its functional form, have any relevant observable impact.

Acknowledgements This work is supported by STFC, through Grants Nos ST/L005743/1 and ST/P005314/1; by grant PID2020-118758GB-I00 funded by MCIN/AEI/10.13039/501100011033; by the “Ramón y Cajal” grant RYC2018-026072 funded by MCIN/AEI /10.13039/501100011033 and FSE “El FSE invierte en tu futuro”; by the “Unit of Excellence María de Maeztu 2020-2023” award to the Institute of Cosmos Sciences, funded by MCIN/AEI/10.13039/501100011033; and by TRIUMF, which receives federal funding via a contribution agreement with the National Research Council of Canada.

Funding Information Open Access funding provided thanks to the CRUE-CSIC agreement with Springer Nature.

Data Availability Statement This manuscript has associated data in a data repository. [Authors’ comment: The data is available in the github repository [83].]

Open Access This article is licensed under a Creative Commons Attribution 4.0 International License, which permits use, sharing, adaptation, distribution and reproduction in any medium or format, as long as you give appropriate credit to the original author(s) and the source, provide a link to the Creative Commons licence, and indicate if changes were made. The images or other third party material in this article are included in the article’s Creative Commons licence, unless indicated otherwise in a credit line to the material. If material is not included in the article’s Creative Commons licence and your intended use is not permitted by statutory regulation or exceeds the permitted use, you will need to obtain permission directly from the copyright holder. To view a copy of this licence, visit <http://creativecommons.org/licenses/by/4.0/>.

Appendix A: Numerical fits

The numerical fits have been performed with Python’s `scipy.optimize.curve_fit` routine [82], which performs a non-linear least squares fit of data to a function. We use the non-zero values of Δ_0 and T_c , as well as their errors, in the fit. The data and fit routines are available in `github` [83].

As a measure of the quality of the fit, we use the absolute value of the maximum deviation from the data centroids to the fits, r_{\max} . This is small for the more precise and abundant BCS+HF data, with values $r_{\max}^{\Delta_0} = 0.01$ MeV ($r_{\max}^{T_c} = 0.04$ MeV) and $r_{\max}^{\Delta_0} = 0.01$ MeV ($r_{\max}^{T_c} = 0.05$ MeV) for the EM and EM+3NF gap (T_c) data, respectively. In contrast, the SRC data is more noisy and the fit has lower quality. The maximum deviations for all quantities and potentials in this case is $r_{\max}^x = 0.04$ MeV.

References

1. P. Haensel, A.Y. Potekhin, D.G. Yakovlev, *Neutron Stars 1: Equation of State and Structure* (Springer, Berlin, 2007)
2. S.L. Shapiro, S.A. Teukolsky, *Black Holes, White Dwarfs, and Neutron Stars: The Physics of Compact Objects* (Wiley Online Library, Hoboken, 1983)
3. C.W. Misner, K.S. Thorne, J.A. Wheeler, *Gravitation* (W.H. Freeman, New York, 1973)
4. A.W. Steiner, J.M. Lattimer, E.F. Brown, The neutron star mass-radius relation and the equation of state of dense matter. *Astrophys. J.* **765**(1), L5 (2013). <https://doi.org/10.1088/2041-8205/765/1/L5>, [arXiv:1205.6871](https://arxiv.org/abs/1205.6871)
5. J.M. Lattimer, The nuclear equation of state and neutron star masses. *Annu. Rev. Nucl. Part. S.* **62**(1), 485–515 (2012). <https://doi.org/10.1146/annurev-nucl-102711-095018>. [arXiv:1305.3510](https://arxiv.org/abs/1305.3510)
6. F. Özel, P. Freire, Masses, radii, and the equation of state of neutron stars. *Annu. Rev. Astron. Astr.* **54**(1), 401–440 (2016). <https://doi.org/10.1146/annurev-astro-081915-023322>. [arXiv:1603.02698](https://arxiv.org/abs/1603.02698)
7. P.B. Demorest, T. Pennucci, S.M. Ransom, M.S.E. Roberts, J.W.T. Hessels, A two-solar-mass neutron star measured using Shapiro delay. *Nature* **467**(7319), 1081–1083 (2010). <https://doi.org/10.1038/nature09466>, arxiv.org/abs/1010.5788
8. H.T. Cromartie, E. Fonseca, S.M. Ransom, P.B. Demorest, Z. Arzumanyan, H. Blumer, P.R. Brook, M.E. DeCesar, T. Dolch, J.A.

- Ellis, R.D., Ferdman, E.C., Ferrara, N., Garver-Daniels, P.A., Gentile, M.L., Jones, M.T., Lam, D.R., Lorimer, R.S., Lynch, M.A., McLaughlin, C. Ng, D.J., Nice, T.T., Pennucci, R., Spiewak, I.H., Stairs, K., Stovall, J.K., Swiggum, W.W., Zhu, Relativistic Shapiro delay measurements of an extremely massive millisecond pulsar. *Nat. Astron.* **4**(1), 72–76 (2020). <https://doi.org/10.1038/s41550-019-0880-2>. arXiv:1904.06759
9. E. Fonseca, H.T. Cromartie, T.T. Pennucci, P.S. Ray, A.Y. Kirichenko, S.M. Ransom, P.B. Demorest, I.H. Stairs, Z. Arzoumanian, L. Guillemot, A. Parthasarathy, M. Kerr, I. Cognard, P.T. Baker, H. Blumer, P.R. Brook, M. DeCesar, T. Dolch, F.A. Dong, E.C. Ferrara, W. Fiore, N. Garver-Daniels, D.C. Good, R. Jennings, M.L. Jones, V.M. Kaspi, M.T. Lam, D.R. Lorimer, J. Luo, A. McEwen, J.W. McKee, M.A. McLaughlin, N. Mann, B.W. Meyers, A. Naidu, C. Ng, D.J. Nice, N. Pol, H.A. Radovan, B. Shapiro-Albert, C.M. Tan, S.P. Tendulkar, J.K. Swiggum, H.M. Wahl, W.W. Zhu, Refined mass and geometric measurements of the high-mass PSR J0740+6620. *Astrophys. J. Lett.* **915**(1), L12 (2021). <https://doi.org/10.3847/2041-8213/ac03b8>. arXiv:2104.00880
 10. J.M. Lattimer, A.W. Steiner, Neutron star masses and radii from quiescent low-mass X-ray binaries. *Astrophys. J.* **784**(2), 123 (2014). <https://doi.org/10.1088/0004-637X/784/2/123>. arXiv:1305.3242
 11. G. Raaijmakers, S.K. Greif, K. Hebeler, T. Hinderer, S. Nisanke, A. Schwenk, T.E. Riley, A.L. Watts, J.M. Lattimer, W.C.G. Ho, Constraints on the dense matter equation of state and neutron star properties from NICER's mass-radius estimate of psr j0740+6620 and multimessenger observations. *Astrophys. J. Lett.* **918**(2), L29 (2021). <https://doi.org/10.3847/2041-8213/ac089a>. arXiv:2105.06981
 12. B.P. Abbott et al., GW170817: observation of gravitational waves from a binary neutron star inspiral. *Phys. Rev. Lett.* **119**, 16 (2017). <https://doi.org/10.1103/PhysRevLett.119.161101>, arXiv:1710.05836
 13. B.P. Abbott et al., GW170817: measurements of neutron star radii and equation of state. *Phys. Rev. Lett.* **121**, 16 (2018). <https://doi.org/10.1103/PhysRevLett.121.161101>, arXiv:1805.11581
 14. B.P. Abbott et al., Properties of the binary neutron star merger GW170817. *Phys. Rev. X* **9**(1), 011001 (2019). <https://doi.org/10.1103/PhysRevX.9.011001>, arXiv:1805.11579
 15. J.S. Read, B.D. Lackey, B.J. Owen, J.L. Friedman, Constraints on a phenomenologically parametrized neutron-star equation of state. *Phys. Rev. D* **79**, 12 (2009). <https://doi.org/10.1103/PhysRevD.79.124032>, arXiv:0812.2163
 16. M. Oertel, M. Hempel, T. Klöhn, S. Typel, Equations of state for supernovae and compact stars. *Rev. Mod. Phys.* **89**, 25 (2017). <https://doi.org/10.1103/RevModPhys.89.015007>, arXiv:1610.03361
 17. CompOSE: Compstar Online Supernovae Equations of State (2022), <https://compose.obspm.fr/>. Accessed 10 Jan 2022
 18. R. Tamagaki, Superfluid state in neutron star matter. I. *Prog. Theor. Phys.* **44**(4), 905–928 (1970). <https://doi.org/10.1143/PTP.44.905>
 19. D. Pines, M.A. Alpar, Superfluidity in neutron stars. *Nature* **316**(6023), 27–32 (1985). <https://doi.org/10.1038/316027a0>
 20. D.J. Dean, M. Hjorth-Jensen, Pairing in nuclear systems: from neutron stars to finite nuclei. *Rev. Mod. Phys.* **75**(2), 607–656 (2003). <https://doi.org/10.1103/RevModPhys.75.607>. arXiv:nucl-th/0210033
 21. N. Chamel, Crustal entrainment and pulsar glitches. *Phys. Rev. Lett.* **110**(1), 011101 (2013). <https://doi.org/10.1103/PhysRevLett.110.011101>. arXiv:1210.8177
 22. D.G. Yakovlev, C.J. Pethick, Neutron star cooling. *Annu. Rev. Astron. Astr.* **42**(1), 169 (2004). <https://doi.org/10.1146/annurev.astro.42.053102.134013>. arXiv:astro-ph/0402143
 23. D. Page, M. Prakash, J.M. Lattimer, A.W. Steiner, Rapid cooling of the neutron star in Cassiopeia A triggered by neutron superfluidity in dense matter. *Phys. Rev. Lett.* **106**(8), 081101 (2011). <https://doi.org/10.1103/PhysRevLett.106.081101> arXiv:1011.6142
 24. P.S. Shternin, D.G. Yakovlev, C.O. Heinke, W.C.G. Ho, D.J. Patnaude, Cooling neutron star in the Cassiopeia A supernova remnant: evidence for superfluidity in the core. *Mon. Not. R. Astron. Soc.* **412**(1), L108–L112 (2011). <https://doi.org/10.1111/j.1745-3933.2011.01015.x>. arXiv:1012.0045
 25. K.G. Elshamouty, C.O. Heinke, G.R. Sivakoff, W.C.G. Ho, P.S. Shternin, D.G. Yakovlev, D.J. Patnaude, L. David, Measuring the cooling of the neutron star in Cassiopeia A with all Chandra X-ray observatory detectors. *Astrophys. J.* **777**(1), 22 (2013). <https://doi.org/10.1088/0004-637X/777/1/22>, arXiv:1306.3387
 26. B. Posselt, G.G. Pavlov, Upper limits on the rapid cooling of the central compact object in Cas A. *Astrophys. J.* **864**(2), 135 (2018). <https://doi.org/10.3847/1538-4357/aad7fc> arXiv:1808.00531
 27. M.J.P. Wijngaarden, W.C.G. Ho, P. Chang, C.O. Heinke, D. Page, M. Beznogov, D.J. Patnaude, Diffusive nuclear burning in cooling simulations and application to new temperature data of the Cassiopeia A neutron star. *Mon. Not. R. Astron. Soc.* **484**(1), 974–988 (2019). <https://doi.org/10.1093/mnras/stz042>. arXiv:1901.01012
 28. W.C.G. Ho, Y. Zhao, C.O. Heinke, D.L. Kaplan, P.S. Shternin, M.J.P. Wijngaarden, X-ray bounds on cooling, composition, and magnetic field of the Cassiopeia A neutron star and young central compact objects. *Mon. Not. R. Astron. Soc.* **506**(4), 5015–5029 (2021). <https://doi.org/10.1093/mnras/stab2081>. arXiv:2107.08060
 29. S. Gandolfi, A. Gezerlis, J. Carlson, Neutron matter from low to high density. *Annu. Rev. Nucl. Part. S* **65**(1), 303–328 (2015). <https://doi.org/10.1146/annurev-nucl-102014-021957>. arXiv:1501.05675
 30. S. Gandolfi, G. Palkanoglou, J. Carlson, A. Gezerlis, K. E. Schmidt, The 1S0 pairing gap in neutron matter. *Cond. Mat.* **7**, 1 (2022). <https://doi.org/10.3390/condmat7010019>, arXiv:2201.01308
 31. W.C.G. Ho, K.G. Elshamouty, C.O. Heinke, A.Y. Potekhin, Tests of the nuclear equation of state and superfluid and superconducting gaps using the Cassiopeia A neutron star. *Phys. Rev. C* **91**(1), 015806 (2015). <https://doi.org/10.1103/PhysRevC.91.015806>. arXiv:1412.7759
 32. C. Drischler, R. Furnstahl, J. Melendez, D. Phillips, How well do we know the neutron-matter equation of state at the densities inside neutron stars? A bayesian approach with correlated uncertainties. *Phys. Rev. Lett.* **125**, 20 (2020). <https://doi.org/10.1103/PhysRevLett.125.202702>, arXiv:2004.07232
 33. A.A. Abrikosov, L.P. Gorkov, I.Y. Dzyaloshinskii, *Quantum Field Theoretical Methods in Statistical Physics*, 2nd edn. (Pergamon Press, London, 1965)
 34. M. Hoffberg, A.E. Glassgold, R.W. Richardson, M. Ruderman, Anisotropic superfluidity in neutron star matter. *Phys. Rev. Lett.* **24**, 775–777 (1970). <https://doi.org/10.1103/PhysRevLett.24.775>
 35. L. Amundsen, E. Østgaard, Superfluidity of neutron matter: (II). Triplet pairing. *Nucl. Phys. A* **442**(1), 163–188 (1985). [https://doi.org/10.1016/0375-9474\(85\)90140-X](https://doi.org/10.1016/0375-9474(85)90140-X)
 36. M. Baldo, O. Elgarøy, L. Engvik, M. Hjorth-Jensen, H.-J. Schulze, 3P_2 – 3F_2 pairing in neutron matter with modern nucleon-nucleon potentials. *Phys. Rev. C* **58**, 1921–1928. (1998). <https://doi.org/10.1103/PhysRevC.58.1921>, arXiv:nucl-th/9806097
 37. V.A. Khodel, J.W. Clark, M. Takano, M.V. Zverev, Phase transitions in nucleonic matter and neutron-star cooling. *Phys. Rev. Lett.* **93**, 151101 (2004). <https://doi.org/10.1103/PhysRevLett.93.151101>, arXiv:astro-ph/0402514
 38. A. Rios, A. Polls, W.H. Dickhoff, Pairing and short-range correlations in nuclear systems. *J. Low Temp. Phys.* **189**(5–6), 234–249 (2017). <https://doi.org/10.1007/s10909-017-1818-7>, arXiv:1707.04140
 39. C. Drischler, T. Krüger, K. Hebeler, A. Schwenk, Pairing in neutron matter: new uncertainty estimates and three-body forces.

- Phys. Rev. C **95**, 5 (2017). <https://doi.org/10.1103/PhysRevC.95.024302>, [arXiv:1610.05213](https://arxiv.org/abs/1610.05213)
40. P. Magierski, G. Wlazlowski, A. Bulgac, Onset of a Pseudogap Regime in Ultracold Fermi Gases. *Physical Review Letters* **107**, 5 (2011). <https://doi.org/10.1103/PhysRevLett.107.145304>, [arXiv:1103.4382](https://arxiv.org/abs/1103.4382)
 41. I. Boettcher, J.M. Pawłowski, C. Wetterich, Critical temperature and superfluid gap of the unitary fermi gas from functional renormalization. *Phys. Rev. A* **89**, 5 (2014). <https://doi.org/10.1103/PhysRevA.89.053630>, arxiv.org/abs/1010.5788
 42. Y.-M. Wu, A. Abanov, A.V. Chubukov, Pairing in quantum critical systems: transition temperature, pairing gap, and their ratio. *Phys. Rev. B* **99**, 014502 (2019). <https://doi.org/10.1103/PhysRevB.99.014502>, [arXiv:1811.02087](https://arxiv.org/abs/1811.02087)
 43. N. Harrison, M.K. Chan, Magic gap ratio for optimally robust superconductivity and its implications for high- T_c (2021), [http://arxiv.org/abs/2110.14785](https://arxiv.org/abs/2110.14785)
 44. A. Richie-Halford, J.E. Drut, A. Bulgac, Emergence of a Pseudogap in the BCS-BEC Crossover. *Phys. Rev. Lett.* **125**, 060403 (2020). <https://doi.org/10.1103/PhysRevLett.125.060403>, [arXiv:2004.05014](https://arxiv.org/abs/2004.05014)
 45. E. Epelbaum, H.-W. Hammer, U.-G. Meißner, Modern theory of nuclear forces. *Rev. Mod. Phys.* **81**, 1773–1825 (2009). <https://doi.org/10.1103/RevModPhys.81.1773>, [arXiv:0811.1338](https://arxiv.org/abs/0811.1338)
 46. C. Drischler, J. Holt, C. Wellenhofer, Chiral effective field theory and the high-density nuclear equation of state. *Annu. Rev. Nucl. Part. S.* **71**(1), 403–432 (2021). <https://doi.org/10.1146/annurev-nucl-102419-041903>, [arXiv:2101.01709](https://arxiv.org/abs/2101.01709)
 47. S. Bogner, R.J. Furnstahl, A. Schwenk, From low-momentum interactions to nuclear structure. *Prog. Part. Nucl. Phys.* **65**(1), 94–147 (2010). <https://doi.org/10.1016/j.pnpnp.2010.03.001>, [arXiv:0912.3688](https://arxiv.org/abs/0912.3688)
 48. M. Baldo, Nuclear methods and the nuclear equation of state. *World Sci.* **1999**, 5 (1999). <https://doi.org/10.1142/2657>
 49. H. Mütter, A. Polls, Two-body correlations in nuclear systems. *Prog. Part. Nucl. Phys.* **45**(1), 243–334 (2000). [https://doi.org/10.1016/S0146-6410\(00\)00105-8](https://doi.org/10.1016/S0146-6410(00)00105-8), [arXiv:nucl-th/0001007](https://arxiv.org/abs/nucl-th/0001007)
 50. M. Baldo, A. Polls, A. Rios, H.-J. Schulze, I. Vidaña, Comparative study of neutron and nuclear matter with simplified Argonne nucleon-nucleon potentials. *Phys. Rev. C* **86**, 064001 (2012). <https://doi.org/10.1103/PhysRevC.86.064001>, [arXiv:1207.6314](https://arxiv.org/abs/1207.6314)
 51. V. Khodel, V. Khodel, J. Clark, Triplet pairing in neutron matter. *Nucl. Phys. A* **679**(3–4), 827–867 (2001). [https://doi.org/10.1016/S0375-9474\(00\)00351-1](https://doi.org/10.1016/S0375-9474(00)00351-1), [arXiv:nucl-th/0001006](https://arxiv.org/abs/nucl-th/0001006)
 52. C. Shen, U. Lombardo, P. Schuck, W. Zuo, N. Sandulescu, Screening effects on $1S_0$ pairing in neutron matter. *Phys. Rev. C* **67**, 6 (2003). <https://doi.org/10.1103/PhysRevC.67.061302>, [arXiv:nucl-th/0212027](https://arxiv.org/abs/nucl-th/0212027)
 53. C. Shen, U. Lombardo, P. Schuck, Screening of nuclear pairing in nuclear and neutron matter. *Phys. Rev. C* **71**, 054301 (2005). <https://doi.org/10.1103/PhysRevC.71.054301>, [arXiv:nucl-th/0503008](https://arxiv.org/abs/nucl-th/0503008)
 54. L.G. Cao, U. Lombardo, P. Schuck, Screening effects in superfluid nuclear and neutron matter within Brueckner theory. *Phys. Rev. C* **74**(6), 064301 (2006). <https://doi.org/10.1103/PhysRevC.74.064301>, [arXiv:nucl-th/0608005](https://arxiv.org/abs/nucl-th/0608005)
 55. A. Schwenk, B. Friman, G.E. Brown, Renormalization group approach to neutron matter: quasiparticle interactions, superfluid gaps and the equation of state. *Nucl. Phys. A* **713**(1–2), 191 (2003). [https://doi.org/10.1016/S0375-9474\(02\)01290-3](https://doi.org/10.1016/S0375-9474(02)01290-3), [arXiv:hep-ph/0207004](https://arxiv.org/abs/hep-ph/0207004)
 56. A. Schwenk, B. Friman, Polarization contributions to the spin dependence of the effective interaction in neutron matter. *Phys. Rev. Lett.* **92**(8), 082501 (2004). <https://doi.org/10.1103/PhysRevLett.92.082501>, [arXiv:nucl-th/0307089](https://arxiv.org/abs/nucl-th/0307089)
 57. D. Ding, A. Rios, H. Dussan, W.H. Dickhoff, S.J. Witte, A. Carbone, A. Polls, Pairing in high-density neutron matter including short- and long-range correlations. *Phys. Rev. C* **94**(2), 025802 (2016). <https://doi.org/10.1103/PhysRevC.94.025802>, [arXiv:1502.05673](https://arxiv.org/abs/1502.05673)
 58. M. Drissi, A. Rios, C. Barbieri, Nambu-covariant many-body theory I: perturbative approximations (2021), [arXiv:2107.09759](https://arxiv.org/abs/2107.09759)
 59. M. Drissi, A. Rios, C. Barbieri, Nambu-covariant many-body theory II: self-consistent approximations (2021), [arXiv:2107.09763](https://arxiv.org/abs/2107.09763)
 60. W. Dickhoff, C. Barbieri, Self-consistent Green's function method for nuclei and nuclear matter. *Prog. Part. Nucl. Phys.* **52**(2), 377–496 (2004). <https://doi.org/10.1016/j.pnpnp.2004.02.038>, arxiv.org/abs/nucl-th/0402034
 61. A. Rios, Green's function techniques for infinite nuclear systems. *Front. Phys. (Lausanne)* **8**, 387 (2020). <https://doi.org/10.3389/fphy.2020.00387>, [arXiv:2006.10610](https://arxiv.org/abs/2006.10610)
 62. H. Mütter, W.H. Dickhoff, Pairing properties of nucleonic matter employing dressed nucleons. *Phys. Rev. C* **72**, 054313 (2005). <https://doi.org/10.1103/PhysRevC.72.054313>, [arXiv:nucl-th/0508035](https://arxiv.org/abs/nucl-th/0508035)
 63. P. Ring, P. Schuck, *The Nuclear Many-Body Problem* (Springer, Berlin, Heidelberg, 1980)
 64. J.R. Engelbrecht, M. Randeria, C.A.R. Sá de Melo, BCS to Bose crossover: broken-symmetry state. *Phys. Rev. B* **55**, 15153–15156 (1997). <https://doi.org/10.1103/PhysRevB.55.15153>
 65. J. Maly, B. Jankó, K. Levin, Numerical studies of the s-wave pseudogap state and related t_c : the “pairing approximation” theory. *Phys. Rev. C* **321**(1), 113–133 (1999). [https://doi.org/10.1016/S0921-4534\(99\)00326-3](https://doi.org/10.1016/S0921-4534(99)00326-3), [arXiv:cond-mat/9805018](https://arxiv.org/abs/cond-mat/9805018)
 66. S. Tsuchiya, R. Watanabe, Y. Ohashi, Single-particle properties and pseudogap effects in the BCS-BEC crossover regime of an ultracold Fermi gas above T_c . *Phys. Rev. A* **80**, 033613 (2009). <https://doi.org/10.1103/PhysRevA.80.033613>, [arXiv:0907.4595](https://arxiv.org/abs/0907.4595)
 67. D.R. Entem, R. Machleidt, Accurate charge-dependent nucleon-nucleon potential at fourth order of chiral perturbation theory. *Phys. Rev. C* **68**, 041001 (2003). <https://doi.org/10.1103/PhysRevC.68.041001>
 68. J.W. Holt, N. Kaiser, W. Weise, Density-dependent effective nucleon-nucleon interaction from chiral three-nucleon forces. *Phys. Rev. C* **81**(2), 024002 (2010). <https://doi.org/10.1103/PhysRevC.81.024002>, [arXiv:0910.1249](https://arxiv.org/abs/0910.1249)
 69. A. Carbone, A. Polls, A. Rios, Symmetric nuclear matter with chiral three-nucleon forces in the self-consistent green's functions approach. *Phys. Rev. C* **88**, 044302 (2013). <https://doi.org/10.1103/PhysRevC.88.044302>, [arXiv:1307.1889](https://arxiv.org/abs/1307.1889)
 70. A. Carbone, A. Cipollone, C. Barbieri, A. Rios, A. Polls, Self-consistent Green's functions formalism with three-body interactions. *Phys. Rev. C* **88**, 054326 (2013). <https://doi.org/10.1103/PhysRevC.88.054326>, [arXiv:1310.3688](https://arxiv.org/abs/1310.3688)
 71. S. Ramanan, M. Urban, BEC-BCS crossover in neutron matter with renormalization-group-based effective interactions. *Phys. Rev. C* **88**, 054315 (2013). <https://doi.org/10.1103/PhysRevC.88.054315>, [arXiv:1308.0939](https://arxiv.org/abs/1308.0939)
 72. W.H. Dickhoff, D. Van Neck, *Many-Body Theory Exposed!*, 2nd edn. (World Scientific, New Jersey, 2008)
 73. G. Stefanucci, R. van Leeuwen, *Nonequilibrium Many-Body Theory of Quantum Systems* (Cambridge University Press, Cambridge, 2013)
 74. P. Božek, Self-consistent solution of Galitskii-Feynman equations at finite temperature. *Phys. Rev. C* **59**, 2619–2626 (1999). <https://doi.org/10.1103/PhysRevC.59.2619>, [arXiv:nucl-th/9811073](https://arxiv.org/abs/nucl-th/9811073)
 75. T. Frick, H. Mütter, Self-consistent solution to the nuclear many-body problem at finite temperature. *Phys. Rev. C* **68**, 034310 (2003). <https://doi.org/10.1103/PhysRevC.68.034310>, [arXiv:nucl-th/0306009](https://arxiv.org/abs/nucl-th/0306009)
 76. A. Ramos, A. Polls, W. Dickhoff, Single-particle properties and short-range correlations in nuclear matter. *Nucl. Phys. A* **503**(1), 1–52 (1989). [https://doi.org/10.1016/0375-9474\(89\)90252-2](https://doi.org/10.1016/0375-9474(89)90252-2)

77. P. Božek, Reduction of the superfluid gap by scattering. *Phys. Rev. C* **62**(5), 054316 (2000). <https://doi.org/10.1103/PhysRevC.62.054316>, [arXiv:nucl-th/0003048](https://arxiv.org/abs/nucl-th/0003048)
78. A. Schirotzek, Y.-I. Shin, C.H. Schunck, W. Ketterle, Determination of the superfluid gap in atomic Fermi gases by quasiparticle spectroscopy. *Phys. Rev. Lett.* **101**, 140403 (2008). <https://doi.org/10.1103/PhysRevLett.101.140403>, [arXiv:0808.0026](https://arxiv.org/abs/0808.0026)
79. M.J.H. Ku, A.T. Sommer, L.W. Cheuk, M.W. Zwierlein, Revealing the superfluid lambda transition in the universal thermodynamics of a unitary Fermi gas. *Science* **335**(6068), 563–567 (2012). <https://doi.org/10.1126/science.1214987>, [arXiv:1110.3309](https://arxiv.org/abs/1110.3309)
80. M. Randeria, E. Taylor, Crossover from Bardeen-Cooper-Schrieffer to Bose-Einstein Condensation and the Unitary Fermi Gas. *Annu. Rev. Cond. Matt. Phys.* **5**, 209–232 (2014). <https://doi.org/10.1146/annurev-conmatphys-031113-133829>, [arXiv:1306.5785](https://arxiv.org/abs/1306.5785)
81. H.-J. Schulze, A. Polls, A. Ramos, Pairing with polarization effects in low-density neutron matter. *Phys. Rev. C* **63**, 044310 (2001). <https://doi.org/10.1103/PhysRevC.63.044310>
82. P. Virtanen, R. Gommers, T. E. Oliphant, M. Haberland, T. Reddy, D. Cournapeau, E. Burovski, P. Peterson, W. Weckesser, J. Bright, S. J. van der Walt, M. Brett, J. Wilson, K. J. Millman, N. Mayorov, A. R. J. Nelson, E. Jones, R. Kern, E. Larson, C. J. Carey, Í. Polat, Y. Feng, E. W. Moore, J. VanderPlas, D. Laxalde, J. Perktold, R. Cimrman, I. Henriksen, E. A. Quintero, C. R. Harris, A. M. Archibald, A. H. Ribeiro, F. Pedregosa, P. van Mulbregt, SciPy 1.0 Contributors, SciPy 1.0: fundamental algorithms for scientific computing in python. *Nature Methods* **17**, 261–272 (2020). <https://doi.org/10.1038/s41592-019-0686-2>
83. GitHub Repository (2022), https://github.com/arnaurios/Gap_Tc_Paper. Accessed 03 Feb 2022